Computers and Electronics in Agriculture 180 (2021) 105882

Contents lists available at ScienceDirect

Computers and Electronics in Agriculture

journal homepage: www.elsevier.com/locate/compag

Improving TLS-based stem volume estimates by field measurements

Timo P. Pitkänen [a,*], Pasi Raumonen [b], Xinlian Liang [c], Matti Lehtomäki [c], Annika Kangas [d]

[a] Natural Resources Institute Finland (Luke), Latokartanonkaari 9, FI-00790 Helsinki, Finland
[b] Mathematics, Tampere University, Korkeakoulunkatu 7, FI-33720 Tampere, Finland
[c] Finnish Geospatial Research Institute FGI, The National Land Survey of Finland, Geodeetinrinne 2, FI-02430 Masala, Finland
[d] Natural Resources Institute Finland (Luke), Yliopistokatu 6 B, FI-80100 Joensuu, Finland

A B S T R A C T

The prediction of tree stem volumes has conventionally been based on simple field measurements and applicable allometric functions, but terrestrial laser scanning (TLS) has enabled new opportunities for extracting stem volumes of single trees. TLS-based tree dimensions are commonly estimated by automatized cylinder- or circle-based fitting approaches which, given that the stem cross-sections are relatively round and the whole stem is sufficiently covered by TLS points, enable an accurate prediction of the stem volume. The results are, however, often deteriorated by co-registration errors and occlusions, i.e., incompletely visible parts of the stem, which easily lead to poorly fitted features and problems in locating the actual treetop. As these defects are difficult to be controlled or totally avoided when collecting data at a plot level, taking advantage of additional field measurements is proposed to improve the fitting process and mitigate gross errors in the prediction of stem volumes. In this paper, this is demonstrated by modelling the stems first as cylinders by only using TLS data, after which the results are refined with the assistance of field data. The applied data consists of various field-measured stem dimensions which are used to define the acceptable diameter estimation limits and set the correct vertical extents for the analyzed tree. This approach is tested using two data sets, differing in the scanning setup, location, and the measured field variables. Adding field data improves the results and, at best, enables almost unbiased volumetric predictions with an RMSE of less than 5%. According to these results, combining TLS point clouds and simple field measurements has the potential to produce stem volume information at a considerably higher accuracy than TLS data alone.

1. Introduction

Reliable and unbiased measurements on tree stem volumes have important implications for the sustainable planning of forest resources, providing not only data for harvesting decisions but also for helping to estimate the impacts of forestry activities on carbon stock, and further effects on climate regulation (Bonan, 2008; Patenaude, et al., 2005; Vaunkonen and Packalen, 2018; Zianis, et al., 2005). The challenge with stem volumes, however, lies in their measurement: as determining accurate stem dimensions is tedious and prohibitively expensive, a conventional and practical solution is to predict the volumes using allometric equations which require only a few simple parameters, such as diameter at breast height and tree height (Laasasenaho, 1982; West, 2015; Zianis, et al., 2005). While these equations are often regarded as sufficiently accurate for most purposes, the accuracy of the predicted stem volumes is limited by the initially estimated model, and subject to any uncertainties or bias related to the model's applicability to the measured trees (McRoberts & Westfall, 2014; Nölke, et al., 2015). Moreover, any changes in climatic conditions or forest management are likely to have implications in tree form rather than only size, which will alter the allometric relationships and decrease the performance of equations in the long run (Saarinen, et al., 2019a; Schneider, et al., 2018).

The application of new techniques, such as terrestrial laser scanning (TLS), have the potential to improve stem volume estimates. Detecting trees and estimating their dimensions using TLS has recently become more widespread, deriving from its capabilities of augmenting the characterization of forest structure rather than just replicating traditional measurements (Liang, et al., 2016; Liang, et al., 2018; Newnham, et al., 2015; White, et al., 2016). Recently, several studies have indicated that point cloud data can be successfully applied to predict stem volumes at a level of single trees (e.g., Liang, et al., 2014; 2018), which also enables using them for the calibration of the allometric functions (Sun, et al., 2016; Takoudjou, et al., 2018), and further for volume estimation in larger areas (McRoberts & Westfall, 2014). The processing of TLS data starts from a point cloud, i.e., a set of single hits of laser beams, which can be converted into stem diameters or cylinders by using manual evaluation or automatized fitting algorithms (Liang, et al., 2018; Liu, et al., 2018; Pitkänen, et al., 2019; Raumonen, et al., 2015; Reddy, et al., 2018). Voxel-based strategies are used as well to simplify complicated

* Corresponding author.
E-mail address: timo.p.pitkanen@luke.fi (T.P. Pitkänen).

https://doi.org/10.1016/j.compag.2020.105882
Received 1 June 2020; Received in revised form 27 October 2020; Accepted 1 November 2020
Available online 1 December 2020

structures (Grau, et al., 2017; Hauglin, et al., 2013; Heinzel & Huber, 2017a; Hosoi, et al., 2013). Initial data used for feature estimation can consist of a single scan, several individual scans, or a co-registered combination of multiple scans. Although collecting data using multiple scans will increase both fieldwork efforts and the processing time, there is a wide consensus of its superiority through producing higher level of details and suffering fewer occlusion effects compared to single scans (Liang, et al., 2016; Newnham, et al., 2015; Saarinen, et al., 2017; Seidel, et al., 2016).

The performance of allometric functions depends principally on the similarity of the focused trees to the initial model estimation data, as well as the accuracy of the field measurements. For applications using TLS data, however, errors derive from a combination of forest structure, scanning conditions, and limitations in converting the single points into larger features. Structural issues relate primarily to occlusion effects which hinder the visibility of the stem, often leading to erroneously estimated diameters and tree height (Abegg, et al., 2017; Raumonen, et al., 2015; Srinivasan, et al., 2015). These effects are aggravated by an increase in stem density, lush understory vegetation and dense canopy layer, which result in a larger proportion of shaded areas and non-stem returns (Béland, et al., 2014; Kuronen, et al., 2018; Seidel, et al., 2013). Consequently, the stem detection rate also decreases steadily as the structural complexity of the forest increases (Liang, et al., 2018). Scanning conditions, apart from seasonal vegetation changes, are particularly affected by rain and wind. Scanners themselves tend to be reasonably well protected against water, but wet conditions affect the transmission of the laser pulse as well as backscattering properties (Wilkes, et al., 2017). Wind, in turn, does not prohibit scanning as such but causes the displacement of tree structures and easily results in co-registration faults, particularly in the upper parts of the stem (Dassot, et al., 2011; Griebel, et al., 2015; Pitkänen et al. 2019; Pyörälä et al., 2018; Vaaja, et al., 2016).

Limitations of feature extraction derive partly from the scanning technology itself, provided that the data quality is affected by an increased beam divergence and footprint area at further distances from the scanner, as well as ghost points resulting from the beam to intercept multiple objects (Cifuentes, et al., 2014; Forsman, et al., 2018; Heinzel & Huber, 2017b). Larger deviations, however, derive from the noisiness and incompleteness of the point cloud data, as well as from irregularities of the targeted stem. To cope with the potential defects, particularly in automatized analyses, fitting algorithms are normally preceded by a rigorous removal of outlier points, i.e., expected non-stem points (Paláncz, et al., 2016; Pueschel, et al., 2013; Wang, et al., 2017). While this can solve part of the problems, a lack of TLS points due to occlusions, overlapping stem halves deriving from co-registration faults, or strong deviations of the stem from the simplified round shape may easily result in erroneously estimated diameters (Abegg, et al., 2017; Åkerblom, et al., 2015). Single strongly anomalous features may often be easily detected and removed by comparing them to the preceding and following values (Pitkänen, et al., 2019; Saarinen, et al., 2017), but this requires that most estimates are successful, and there are no systematic defects.

To calculate accurate stem volumes using TLS data, but to simultaneously tackle the challenges related to the analysis, a hybrid approach is demonstrated for predicting TLS-based stem volumes, which includes applying a limited number of field measurements. In other words, stem volumes of single trees are derived from using a TLS-based feature extraction procedure. However, instead of relying only on point cloud data, manually measured diameters, tree height and previous knowledge on the stem form are used. This additional data is intended for correcting common errors associated with TLS-derived stem volumes, which result from poorly fitted diameters and under- or overestimated vertical tree dimensions. Volumes are calculated using several combinations, i.e., with and without field measurements, and the results are compared to existing allometric functions. This allows for the identification of the effects of the applied data and the discussion of the benefits of the approach compared to using sole TLS data.

2. Materials and methods

2.1. Source materials

The data used in this study included two distinct sets, referred to later as datasets I and II. **Dataset I** consists of six 32 m × 32 m plots, scanned in 2014 from Evo, Finland (Fig. 1), for the international TLS benchmarking project (Liang, et al., 2018). Scanning was performed without any pre-scan preparations using a Leica HDS6100 in high density mode, giving a point spacing of 15.7 mm at 25 m distance from the scanner. The plots were scanned using five stations, one in the middle and four additional scans in intermediate directions (NW, NE, SW and SE) located theoretically at 11.3 m distance from the plot center, but these locations were allowed to be moved according to plot conditions. Scans were co-registered with an average accuracy of 2.1 mm using six spheroid reference targets put throughout the plot. Only multi-scan data, i.e., a co-registered point cloud of the distinct scans, was applied in this study. The plots were categorized into three forest complexity categories (easy, medium and difficult) depending on the stem density and understory vegetation. Easy plots had minimal understory vegetation and a low stem density (~600 trees/ha), while medium (~1000 trees/ha) and difficult (~2000 trees/ha) had both higher stem densities and denser understory vegetation. Field measurements assisting in the TLS analysis included diameter at breast height (h = 1.3 m; referred to as $d_{1.3}$) and tree height (h_T) measured from all the trees having a $d_{1.3}$ greater than 50 mm. The reference stem volumes were predicted based on diameter measurements between the base and the top of the tree, which were performed manually from the point cloud from heights of 0.65 m, 1.3 m, 2 m and further at one-meter intervals until the treetop. Dataset I contained 651 trees with sufficient visibility to allow for reliable measurements. More details regarding the data acquisition and

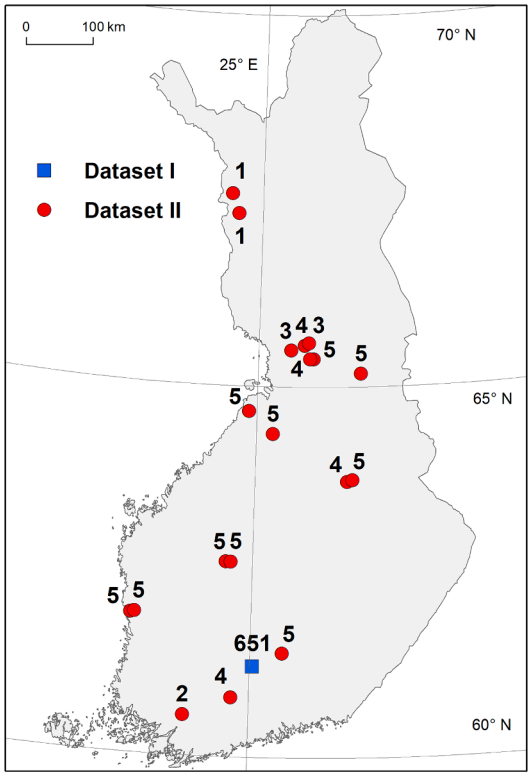

Fig. 1. Locations of sample plots and number of sample trees per plot. For dataset I, plots are located close to each other, and have therefore been combined as one symbol in the map.

processing are provided in Liang et al. (2018).

Dataset II refers to TLS material, scanned by the Natural Resources Institute Finland (Luke) from 18 field plots, located in different parts of Finland (Figs. 1 and 2). Their stem densities ranged from approximately 270 to 3000 trees/ha with a median value of 1200. The plots were selected to include a diverse sample of peatland forests based on their previous measurements within the national forest inventory (NFI) framework. Sampling only on peatland areas was due to other planned uses of the data, but no significant structural variation between forests on peatland and mineral soil from the perspective of TLS analyses was expected to occur. From each plot, a maximum of five sample trees were selected, thus reducing the effects of within-stand correlation and following the sampling strategy used by Laasasenaho (1982) to collect data for stem volume modelling. Sample trees (n = 76) were picked randomly among candidate trees, which were included in an angle count (Bitterlich) plot with a basal area factor of q = 2 (Tomppo, et al., 2011) within a maximum radius of 9.00 m, had a $d_{1.3}$ of 50 mm or more, and were either Scots pine (*Pinus sylvestris*; n = 53), Norway spruce (*Picea abies*; n = 10), silver birch (*Betula pendula*; n = 1) or downy birch (*Betula pubescens*; n = 12). The two birch species were combined at the analysis stage. Furthermore, strong external disturbance factors (e.g., by fungi or insects) or forked trees due to expected earlier stem damages were not allowed for sample trees. Selected sample trees had a $d_{1.3}$ of between 60 and 321 mm (median 155 mm), and an h_T of between 4.5 and 22.1 m (median 13.4 m). The observed species are referred to simply as pine, spruce and birch later in this paper.

The field plots of dataset II were first scanned using a Leica P40 terrestrial laser scanner between April and October in 2018, using 3.1 mm point spacing at 10 m distance. The scans were performed without any pre-scan preparations in dry weather conditions, having temperatures varying between −3 and + 23 degrees C and wind between 1.1 and 6.4 m/s as recorded concurrently in the nearest official weather station. Each plot was scanned using 4–5 stations, which were placed with the intention of ensuring the visibility of the sample trees from several directions. The standard procedure was to place one station in the middle of the sample trees and the others in different directions behind them, but the design was allowed to be adjusted as required to minimize occlusions. The scans were co-registered together using 4–5 spheroid targets, resulting in an average accuracy of 1.0 mm and single target errors of up to 6 mm. Before scanning, all the sample trees were marked with duct tape placed 10 cm above the breast height (1.3 m), thus allowing for later tree identification from the point cloud and providing a reference height without interfering with the measurement of the diameter at h = 1.3 m.

The field measurements from the sample trees were made between July and December in 2018, most of which were made shortly after scanning, but for practical reasons this was not always possible. Given the seasonal dynamics of boreal trees (Henttonen, et al., 2009), on six out of 18 plots some radial increment was likely to have occurred after scanning, but these effects were expected to be minor compared to other potential sources of errors. During the fieldwork, the tree locations and their $d_{1.3}$ were measured, and the species observed from standing sample trees. After that, the trees were felled, followed by measurements of the h_T, the stump height (h_S), the diameter at stump height (d_S) and the diameter at 6 m height (d_6). The diameter d_6 was previously measured in the Finnish NFI and included in the volume functions by Laasasenaho (1982), but this was later removed from the NFI due to the tediousness of measuring it.

The stump height was determined by the uppermost root collar which affected cutting, or at least 10 cm above the ground. Finally, the diameters of each tree at proportional heights of 1, 2.5, 5, 7.5, 10, 15, 20, 30, 40, 50, 60, 70, 80, 85, 90 and 95% were measured, each of which as an averaged value of two opposite directions. These diameters were then used to predict the reference stem volumes between the stump height and the treetop by integrating a cubic spline fitted to the measurements, following the methodology of Laasasenaho (1982).

2.2. Data processing

General approach

TLS processing was a further developed version from Pitkänen et al. (2019) and applied to co-registered point clouds which had been decimated to contain only one point per 5 mm × 5 mm × 5 mm cube. The processing chain consisted of five steps performed using MATLAB 2016b (MATLAB 2016) and R Statistical Software version 3.3.1 (R Core Team 2016) as introduced briefly below:

(1) **Stem detection and cylinder construction**: fully automatic stem detection and cylinder fitting, used to provide the stem structure for the following steps but not applied for the volume calculation per se;
(2) **Vertical adjustment**: detection of the tree base and top by additional procedures, given that cylinder construction is often deficient in the occluded parts of the stem;

Fig. 2. A typical field plot of dataset II, including different tree species and plotwise variation in stem density.

(3) **Reference taper curve**: determination of the expected taper curve and its allowed limits to be applied in the diameter estimation;
(4) **Stem slicing and diameter estimation**: splitting the stem into thin slices and estimating their diameters using a circle fitting approach; and
(5) **Stem volume prediction**: constructing a continuous taper curve based on the estimated diameters and using it for predicting the stem volume.

Two stem volume prediction models were developed for dataset I (I.1 and I.2) and four models for dataset II (II.1–4), deriving from the differences of assisting field measurements and allowing for the evaluation of their importance (Table 1 and Fig. 3). For both data sets, the first model only had a TLS point cloud with no field measurements, while the last included all the available data. Due to a larger range of fieldwork-based variables, two intermediate models were also created for dataset II: one targeted at adjusting only the vertical stem dimensions (II.2) and the other including all the available variables except the d_6 (II.3). The principal uses of the field data are summarized in Table 2.

2.3. Stem detection and cylinder construction

Stem detection and cylinder construction included three main steps, which are described in more detail in Pitkänen et al. (2019). The first step was to filter the decimated point cloud and estimate the ground level using a grid of 25 cm × 25 cm horizontal squares. Points near to the ground as well as low-density parts of the point cloud were removed. In the second step, the filtered point cloud was covered with small sets, or surface patches, having diameters of about 5–10 cm. The neighbours and surface normal of these sets were also estimated. In the third step, the stems were iteratively isolated and modelled as cylinders. The initial stem sections were identified as a connected collection of nearly vertical surface patches (i.e., having horizontal surface normals), which were further tested for a cylinder fit. Then, the approved sections were expanded into full stems; first until the ground level and then towards the treetop. The expansion was based on iteratively fitting cylinders of different lengths, if necessary, to find a cylinder part to continue the stem. In addition, when a whole stem was finally isolated, its surface points were excluded from other potential stems to be detected for later iterations.

Each plot was processed five times, given that there was a potential variation due to random seeds in defining the surface patches and in the stem isolation process. Those stems which were less than 20 cm apart from each other in the distinct modelling attempts, as measured horizontally at h = 1.3 m, were regarded as the same individual. Trees found only in one out of five modelling attempts, having a cumulative stem cylinder length less than 1.35 m, or being regarded as unrealistic (defined as having a stem length of less than 20 × cylinder-measured $d_{1.3}$), were removed. The approved stems were matched with the field-detected trees, and among the distinct cylinder models of each individual, the model having the longest stem was selected to be applied in the following processing steps.

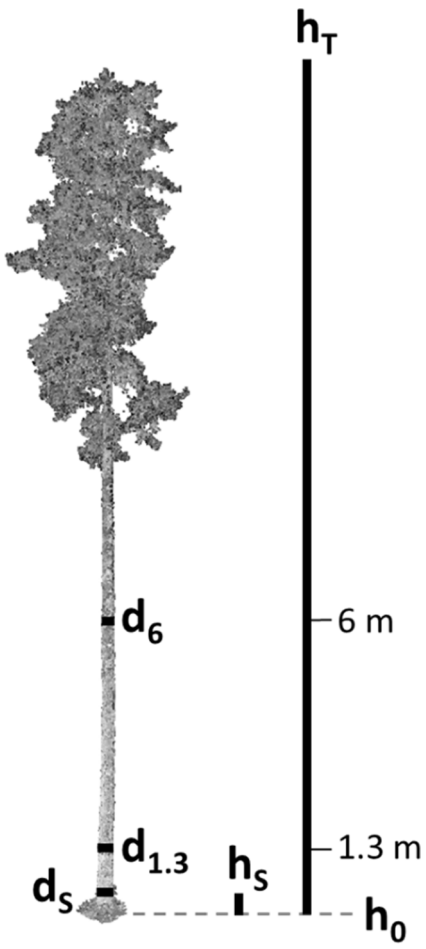

Fig. 3. Schematic presentation of the applied field measurements.

Table 1
Data and field measurements used in the different volume prediction models (as "X").

		DATASET I		DATASET II			
		I.1	I.2	II.1	II.2	II.3	II.4
Point cloud data		X	X	X	X	X	X
FIELD MEASUREMENTS	h_T		X		X	X	X
	h_0 and h_S				X	X	X
	$d_{1.3}$		X			X	X
	d_S and species					X	X
	d_6						X

h_T = tree height.
h_0 = ground level, i.e., tree base.
h_S = stump height.
$d_{1.3}$ = diameter at 1.3 m height.
d_S = diameter at stump height.
d_6 = diameter at 6 m height.

Table 2
Usage of different supplementary data sources.

Variable(s)	Principal use
h_0, h_S and h_T	Vertical adjustment of the stem and correction of height-related errors
Species	Construction of a species-specific reference taper curve for diameter estimation
d_S, $d_{1.3}$ and d_6	Used both for predicting the reference taper curve and the final stem volume

2.4. Vertical adjustment

In models I.1, I.2 and II.1, the h_0 was determined based on the cylinder model and the point cloud. For this purpose, the lowermost cylinder was extended downwards, and the level after which no TLS points existed in the close vicinity of the stem, i.e., within a 100 mm horizontal distance from the cylinder edge, was defined as the h_0. In models II.2–4, duct tape set at h = 1.4 m was automatically detected based on its anomalous TLS-recorded intensity values, thus providing the reference level for the h_0.

The stump height for model II.1 was defined as being 20 cm upwards from the lowermost cylinder start, which was based on earlier data collection experiments. In models II.2–4, the h_S was based on the field-measured value, and in models I.1–2 it was not required at all as the targeted stem volume included the stump part as well.

In models I.1 and II.1, determination of the h_T was based on selecting TLS points above the uppermost cylinder end within a horizontal radius of 2 × cylinder-based $d_{1.3}$ and defining the treetop by the first vertical section of 3 × cylinder-based $d_{1.3}$ with no points. Applying selection ranges based on the $d_{1.3}$ intended at setting lower limits for smaller trees and, therefore, improving the height evaluation of intermediate and suppressed trees. In other models, the h_T was based on the field-measured value.

2.5. Reference taper curve

To reduce the likelihood of under- or overestimated stem diameters at later processing stages, each sample tree was predicted a reference taper curve which defined the allowed diameter limits. This curve was based either on initial cylinders or, if the species was known, on pre-existing information with respect to the targeted species. Of these options, the species-specific taper curve was considered as providing more robust reference data independently of potential cylinder-derived errors, although having a lower potential to analyse highly anomalous stems.

For models I.1–2 and II.1–2 without species data, the initial cylinders and h_T were used for constructing the reference taper curve. The prediction was made by extracting mid-cylinder heights with their respective diameters and adding the h_T with a diameter of zero. As the quality of the diameter estimation decreases further up in the stem due to the longer distance to the scanner and occlusion effects (de Conto et al., 2017; Mengesha, et al., 2015; Pyörälä et al., 2018), only cylinders up to the height of $h_T/2$ were used for this purpose. A cubic spline was fitted to the midpoints and the h_T and final reference limits for the circle fitting phase were defined by the spline-predicted diameter with a tolerance of ± 20%. This appeared to provide the best achievable compromise to reconstruct a rough but relatively realistic reference taper curve.

The reference curves for models II.3 and II.4 were assisted by the earlier field-measured detailed tapering data of 1513 trees from Finland which were derived from VAPU, i.e., the "National Tree Study" (Korhonen & Maltamo, 1990) and digital image measurement (Varjo, et al., 2006) projects. From this data, a subset of 50 trees of the same species and with the most similar $d_{1.3}$ to the tree of interest were selected. No geographical location or site characteristics were considered in this selection to include a higher degree of variation. The earlier data was converted into polar coordinates (Lappi 1986; 2006), and dimensions corresponding to the available field measurements (see Table 1; the h_T was included with a diameter of zero) were linearly interpolated. Then, a set of generalized linear models was estimated to predict the unknown stem dimensions at 12 different heights based on the available field measurements using polar angles of 0.25, 0.7, 1.5, 3, 5, 8, 14, 21, 31, 41, 56 and 72 degrees as suggested by Lappi (1986). Finally, the predicted polar dimensions of the tree of interest were converted back to heights and diameters, followed by constructing the reference taper curve by fitting a cubic spline. The upper and lower limits for diameter prediction were defined using a tolerance of ± 10% (Fig. 4).

2.6. Stem slicing and diameter estimation

For the diameter estimation, the point cloud around the stem was split into thin slices. The slices were extracted at a height of every 10 cm, including TLS points selected initially within a ± 5 mm vertical range, and extending the selection distance both up- and downwards at 5 mm steps if required until reaching 2500 points or a ± 12.5 cm vertical distance. Each slice was then flattened into a horizontal (x,y) projection, followed by a diameter estimation using a RANSAC circle fitting algorithm (Fischler & Bolles, 1981) with 1000 iterations and further approval conditions (Fig. 5). Dataset I allowed a fitting only using the co-registered data, but dataset II, having station identifiers as point attributes, enabled the extraction of individual scans to reduce potential co-registration errors and wind effects.

Each RANSAC iteration was based on selecting three random points from the slice, which were used to draw a circle passing through the points. To be approved as a candidate diameter, the circle was required to be within the diameter limits of the reference taper curve, having none or few TLS points inside, and possessing sufficient point coverage along its edge. The edge width as well as allowed points inside were defined relative to the radius of the reference taper curve (r_{ref}, in metres), thus making them more suitable for stems of different sizes. The edge was defined as a zone within $r_{ref} \pm 0.075 \times r_{ref}$, and the maximum number of points inside was set to 200 × r_{ref} (excluding the edge),

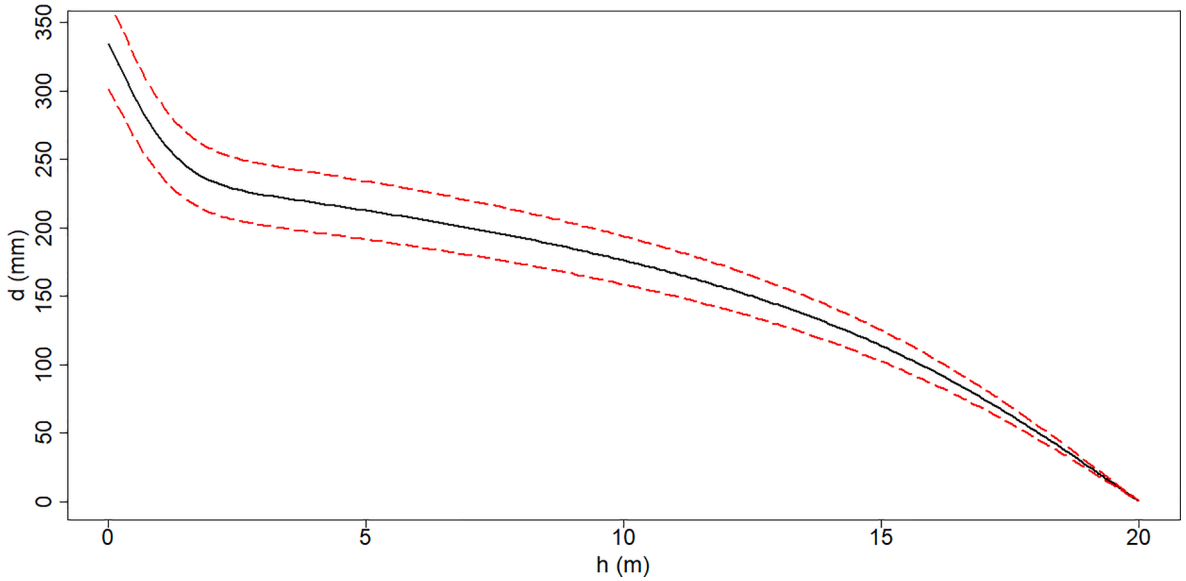

Fig. 4. An example of a reference taper curve (black, solid) with allowed upper and lower limits (red, dashed) constructed for a tree which is known to be a Scots pine, having $d_{1.3}$ = 250 mm and h_T = 20 m.

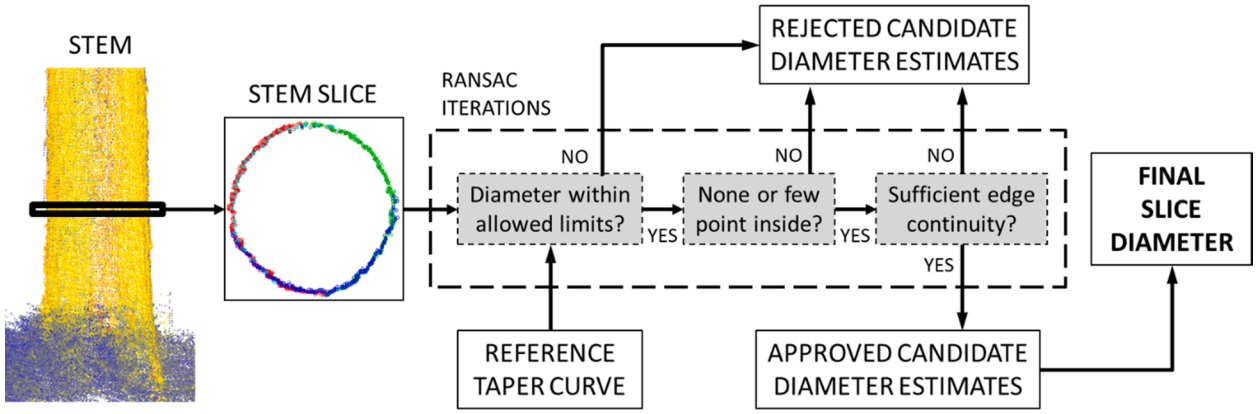

Fig. 5. The process of re-evaluating slice diameters.

according to those limits found suitable in earlier tests for the applied TLS data.

Provided that the first two conditions were satisfied, the edge continuity was determined by dividing the edge into 10 mm long sections and by calculating the proportion of sections including TLS points. Those sections with no adjacent continuity were regarded as noise and discarded. The continuity limits were determined separately for both data sets deriving from their differing characteristics. For dataset I with only co-registered data, a minimum limit of 40% edge continuity was found to be a suitable compromise to maximise circle approval without major defects. For dataset II, almost full circles were first attempted to be found from co-registered data with an edge continuity of 85% or more. If no approved estimate was found, individual scans were extracted, and fitting procedure was repeated with each applying a continuity limit of 33%.

After the RANSAC iterations, the final slice diameter was defined among the approved estimates primarily by the highest edge continuity proportion and secondarily, if several candidates shared the same proportion, by the sum of the edge points' intensity values. Both the larger number of TLS points and their higher intensities were expected to derive from the stem rather than, for example, from foliage or branches due to the larger contact area and relatively perpendicular surface of the stem to the incident beam (Côté, et al., 2009; Lovell, et al., 2011). If no approved estimate had been found, no diameter was assigned to the respective slice.

2.7. Stem volume prediction

After processing all the slices, potentially anomalous diameters, defined as exceeding the mean value of the three preceding (i.e., lower) diameters by more than 10%, were removed. Then, the approved slice diameters were used to predict a taper curve. A minimum limit of 10 approved slice diameters was set for the taper curve and stem volume prediction; otherwise the tree was discarded, and no stem volume was calculated.

The curve was predicted using a cubic spline. The slice diameters were weighted by their edge continuity proportions, and the h_T was added with d = 0 mm using a full weight, i.e., corresponding to 100% edge continuity. The field-measured diameters were also added with full weights when available, and any potentially approved RANSAC-modelled diameters within a vertical distance of ± 20 cm were removed to avoid potential conflicts. Finally, TLS-derived stem volumes between the h_0 and the h_T (dataset I), or between the h_S and the h_T (dataset II) were calculated using Huber's formula at 1 cm sections. For dataset I, the lowest 0.65 m was regarded as a straight cylinder, thus corresponding to the evaluation of Liang et al. (2018).

2.8. Accuracy assessment

Accuracy of the different stem volume models was evaluated using a mean error (ME, i.e., bias; Eq. 1), a relative mean error (ME%; 2), a root-mean-square error (RMSE; 3) and a relative root-mean-square error (RMSE%; 4):

$$ME = \frac{\sum_{i=1}^{n}(\hat{y}_i - y_i)}{n} \quad (1)$$

$$ME\% = 100*\frac{ME}{\bar{y}} \quad (2)$$

$$RMSE = \sqrt{\frac{\sum_{i=1}^{n}(\hat{y}_i - y_i)^2}{n}} \quad (3)$$

$$RMSE\% = 100*\frac{RMSE}{\bar{y}} \quad (4)$$

where n is the number of analysed trees, $\hat{y}_i$ is the stem volume predicted for tree i, y_i is the reference stem volume measured manually for the respective tree, and $\bar{y}$ is the arithmetic mean of all the predicted stem volumes.

The evaluation of models from dataset I was performed plotwise, indicating the differences between the complexity categories. Dataset II, in turn, had only few measured trees per plot but enabled assessment of differences between the tree species and comparing the modelling results to Laasasenaho's (1982) allometric volume functions. Furthermore, statistics related to completeness of extracting all the actual trees were calculated for dataset I according to Liang et al. (2018).

3. Results

The errors and completeness of tree extraction regarding dataset I are presented in tables 3 and 4, and errors related to dataset II in table 5, respectively. The number of accepted trees for dataset II are indicated in Table 5 but no separate table for completeness is provided, as only one Norway spruce ($d_{1.3}$ = 83 mm) and one downy birch ($d_{1.3}$ = 103 mm) were rejected due to a lack of successfully estimated slice diameters. In terms of dataset I, the prediction errors of model I.1 were relatively high, and all the volumetric mean errors were clearly negative (Table 3). Model I.2, which included the field-measured $d_{1.3}$ and h_T, however, made a clear improvement particularly for the relative mean errors, although the volumes were still predominantly underestimated. It is noteworthy, however, that both the ME and RMSE of model I.2 were the highest on those plots categorized as easy, exceeding both the medium and difficult plots.

The completeness of the extracted trees for dataset I (Table 4)

Table 3
Volumetric mean and RMS errors of model predictions as well as mean reference volume of trees related to dataset I (n = 651).

	VARIABLE	Plot 1 (easy)	Plot 2 (easy)	Plot 3 (medium)	Plot 4 (medium)	Plot 5 (difficult)	Plot 6 (difficult)
	Mean vol. (dm^3)	482	233	321	787	665	163
Model I.1	ME (dm^3)	−22.5	−23.3	−19.1	−88.4	−95.6	−13.5
	ME (%)	−4.7	−10.0	−5.9	−11.2	−14.4	−8.3
	RMSE (dm^3)	99.2	40.9	41.4	168.0	246.3	33.6
	RMSE (%)	20.6	17.5	12.9	21.3	37.0	20.6
Model I.2	ME (dm^3)	−11.8	−10.5	1.6	−15.1	2.1	−0.7
	ME (%)	−2.5	−4.5	0.5	−1.9	0.3	−0.4
	RMSE (dm^3)	90.3	30.3	24.9	89.7	67.8	20.7
	RMSE (%)	18.7	13.0	7.8	11.4	10.1	12.7

Table 4
Completeness of the extracted trees calculated for dataset I.

	All trees	Accepted trees	Completeness (%)
Plot 1 (easy)	50	44	88.0
Plot 2 (easy)	84	51	60.7
Plot 3 (medium)	131	76	58.0
Plot 4 (medium)	71	46	64.8
Plot 5 (difficult)	118	47	39.8
Plot 6 (difficult)	197	61	31.0

Table 5
Volumetric ME and RMSE of model predictions as well as mean reference volume of trees related to dataset II (n = 74), including Laasasenaho's (1982) two volume functions.

	VARIABLE	ALL TREES (n = 74)	PINES (n = 53)	SPRUCES (n = 9)	BIRCHES (n = 12)
	Mean vol. (dm^3)	173	172	147	199
Model II.1	ME (dm^3)	−2.3	−2.8	−2	−0.4
	ME (%)	−1.3	−1.6	−1.4	−0.2
	RMSE (dm^3)	11	11.4	4.7	12.3
	RMSE (%)	6.3	6.6	3.2	6.2
Model II.2	ME (dm^3)	−0.4	−0.6	−0.8	0.9
	ME (%)	−0.2	−0.3	−0.5	0.5
	RMSE (dm^3)	11.8	11	3.9	17.6
	RMSE (%)	6.8	6.4	2.6	8.8
Model II.3	ME (dm^3)	2.3	2.7	1.2	1.4
	ME (%)	1.3	1.6	0.8	0.7
	RMSE (dm^3)	9.4	9.1	3.7	13.2
	RMSE (%)	5.4	5.3	2.5	6.6
Model II.4	ME (dm^3)	1.2	1.9	0.2	−0.9
	ME (%)	0.7	1.1	0.1	−0.5
	RMSE (dm^3)	8.4	8.8	3.8	8.8
	RMSE (%)	4.8	5.1	2.6	4.4
Volume function ($d_{1.3}$, h_T)	ME (dm^3)	3.4	4.3	2.3	0.3
	ME (%)	2	2.5	1.6	0.2
	RMSE (dm^3)	17.9	18.9	10.5	17.6
	RMSE (%)	10.3	11	7.1	8.8
Volume function ($d_{1.3}$, d_6, h_T)	ME (dm^3)	−0.8	1.2	−2.4	−8.5
	ME (%)	−0.5	0.7	−1.6	−4.3
	RMSE (dm^3)	12.7	9.6	6.5	23.8
	RMSE (%)	7.3	5.6	4.4	11.9

concerns trees which had first been initially detected by the cylinder modelling and further accepted for volumetric calculation, i.e., having at least 10 successfully estimated slice diameters. The largest difference in completeness lies between the medium and difficult plots. Missing trees derived both from non-detections as well as from initially detected but then rejected trees, resulting in an acceptance of 31–88% of all the reference trees.

Dataset II had considerably smaller errors compared to dataset I, because it included more field-measured variables, enabled extracting the individual scans, and had more stations per areal unit (Table 5). Of the four different prediction models, errors were expectedly largest when only the point cloud and initial cylinder model were used (II.1), and smallest when all the available field data was applied (II.4). All the calculated relative mean errors were within ± 1.6%, but only in model II.1 was the volume of all the tree species underestimated. The RMSE values varied between the different species and were the smallest for spruce in all the models. Model II.4 had an RMSE of below 5% and the largest species-wise had a relative ME of 1.1%. The TLS-based results were also better than Laasasenaho's volume functions, of which the one based on $d_{1.3}$ and h_T had particularly larger errors than any of the TLS measurements.

4. Discussion

Applications relying on TLS data have gradually matured to a stage where the replication of simple field measurements has turned into providing relevant information on more complex dimensions, including stem volumes. While the use of automatized analysis steps will provide feasible options to cope with these often vast data sets, they simultaneously increase the risk of obtaining erroneous or biased results. To reduce the chances for unreliable conclusions, the presented approach of this study relies on including a small number of fieldwork-based dimensions to support the TLS analysis, which are intended principally at guiding the analysis towards manually measured dimensions. Collecting the field data may require additional efforts at a level which is not applicable for all purposes, and they should not always be assumed as highly accurate or unbiased. The capabilities of this additional data to improve the results are, however, clear, and to the authors' knowledge, assisting TLS-based predictions by field measurements has previously been mostly limited to correcting potentially erroneous tree heights (Luoma, et al., 2019; Saarinen, et al., 2019b).

The results of datasets I and II differed from each other, resulting primarily from differing plot designs and available field data, as well as capabilities to extract individual scans for dataset II. For dataset I, the RMS errors of stem volumes without field data assistance were between 12.9% and 37%, which are relatively similar compared to those analyses using co-registered data in the TLS benchmark study (Liang et al. 2018). In case the relatively simple field data was utilized, however, the errors were substantially reduced, and the accuracy of the volume estimates improved. Large errors for model I.1 derived principally from the underestimation of tree heights, affecting particularly the medium and difficult plots. The height assessing technique applied to the TLS data was apparently not optimal for dataset I, and occluded mid-stem parts that caused treetop estimates which were too low. An improvement could be gained by dividing the trees into two size classes similarly to Wang et al. (2019a) and by detecting the heights of larger trees based on the uppermost TLS points rather than observing any lower breaks in the point cloud.

Those remaining negative mean errors in model I.2 were presumably derived from the diameter estimation method, which works best when

the separation of individual scans is possible. Even relatively weak wind induces co-registration faults and increases noise, particularly in the upper part of trees, ranging from minor displacements to totally overlapping stem parts, which interferes with diameter estimation (Dassot, et al., 2012; Pitkänen, et al., 2019; Vaaja, et al., 2016). Given the circle fitting evaluation based on edge continuity and the strict limits for allowed inside points, any overlap or converged stem halves will easily result in approved diameters which are too low, leading to underestimated volumes. Assumedly, these effects were strongest on the easiest plots with the best visibility, i.e., those easier ones, which include more signals also from the upper stem sections. It is also possible that lower stem densities may make the stand more susceptible to wind. In addition, the extractability of individual scans would have likely increased the relatively low acceptance rate of trees for volumetric prediction, particularly for difficult plots.

For dataset II, all the relative RMS errors were below 9%. These results can be considered good as similar automatized TLS-based measurements accuracies vary generally between 6% and 50% depending on the forest complexity, scan setup, and applied volume extraction method (Liang, et al., 2018; Saarinen, et al., 2017). The field data applied to dataset II was related to both dimensions of the individual trees as well as to known characteristics of tree species at the level of the whole population. When only the point cloud and initial cylinders were used in the process (model II.1), the negative ME can largely be explained by difficulties in detecting the correct ground level, stump height and tree height, which generally led to an underestimated stem volume. Correcting these errors resulted in a smaller ME but also a somewhat larger RMSE (II.2), derived expectedly from difficulties to predict correctly the lowest part of the stem for birches. Adding field-measured diameters (II.3–4) decreased the RMSE while species-specific reference taper curves helped to keep the ME at a relatively low level.

In terms of the distinct tree species, birch and pine had larger mean errors than spruce. White birches growing on peatland, where the sample trees had been measured, often have curved butts and other stem defects (Herajärvi, 2001; Verkasalo, 1997). Furthermore, this may had caused potential difficulties to extracting the TLS-based diameters if the actual stem dimensions had deviations from the applied reference trees or their cross-sections were not circular enough. Pines are generally straighter but characterized by relatively rough bark, which may lead to deviations between the field-measured and TLS-predicted diameters, as TLS beams penetrate the cracks while a field-operated caliper will generally neglect them. Spruces, in turn, have fewer deformations and thinner bark, but they are often more heavily occluded by branches which may hinder the TLS-based analyses, particularly at denser stands. However, it should be noted that the data set used was small, and therefore individual trees and even their single estimated diameters may have had a substantial effect on the results.

In general, the effects of occlusions and consequent deficiencies in the feature extraction and stem volume prediction are expected to account for a major part of the remaining errors. As shown in this study and by Liang et al. (2014), minimizing occlusions and covering the targeted trees comprehensively by the point cloud data will easily reduce the volumetric RMS errors below 10%, which corresponds to or exceeds the accuracy of the best available allometric equations. Occlusions, however, derive mainly from the existence of understory foliage and branches, depending on the stem density, tree size and species, and are inherent to the static nature of TLS data collection, thus lacking the potential to be completely removed (Bauwens, et al., 2016; Heinzel & Huber, 2017b). Fully occluded parts of the trees are not recorded in the point cloud data at all, providing no potential for feature estimation or volume prediction. Partial occlusions require a careful decision on the level when the gains (more features extracted) are still expected to exceed the losses (deficient extraction quality deteriorates the overall accuracy). Finding this balance is often case-sensitive and would require more studies to assess applicable strategies.

There are various ways to minimize the occlusion effects prior to the analysis phase by optimizing the location and spacing of scanning stations, scanning in windless conditions and in leaf-off season for deciduous trees, as well as by selecting the most appropriate scanner settings (Abegg, et al., 2017; Béland, et al., 2014; Newnham, et al., 2015; Wilkes, et al., 2017). In particular, the optimization of scanning conditions, however, is not always possible due to practical limitations including, for example, the unavailability of a field crew or shortness of the most applicable time windows. For noisy data, a strategy taking advantage of field measurements may therefore be more applicable, as it efficiently helps to avoid gross errors, although it simultaneously restricts the flexibility of the outcome. These restrictions always need to be determined according to the study conditions and expected variation of the measured trees. Recent studies have also indicated that a further leap in feature extraction accuracy could be achieved by combining TLS data with airborne laser scanning either from an aircraft or a UAV, which enables distinguishing canopy details and upper parts of the stem, but also increases the workload and often reduces the feasibility of data collection (Bazezev, et al., 2018; Béland et al., 2019; Ojoatre, et al., 2019; Wang, et al., 2019b; Yrttimaa, et al. 2020).

While the existing volume functions can be regarded as performing reasonably well for the stems of dataset II, their disadvantage are the limitations posed by the initial estimation data, thus lacking the ability to react to any potential changes on the volume with regard to the parameters, measuring anomalies at a single-tree level, or indicating regional differences in the stem form (Dassot, et al., 2012; McRoberts & Westfall, 2014; Olschofsky, et al., 2016). The reference functions by Laasasenaho (1982) applied in this study are based on data collected in the late 1960 s and early 1970 s and appear to have a somewhat positive mean error in the ($d_{1.3}$, h_T) function. This may potentially be due to changes that occurred in the stem form, the unrepresentative sample selected for dataset II, or dissimilarities of the actual measurements, such as defining the stump height. Of these, however, a considerably smaller mean error with a function including the d_6 would support the theory of the altered stem form with respect to the relationships between the $d_{1.3}$, h_T, and the stem volume, which particularly influences the upper part of the stem. This could plausibly result from a faster tree growth due to ongoing climate change (Schneider, et al., 2018), an impact of atmospheric nitrogen deposition, although gradually declining (From, et al., 2016; Schmitz, et al., 2018), and changes in forest management practices (Finnish Forest Research Institute, 2011). Analyzing this in detail is beyond the reach of this study due to the small number of measured trees, but the TLS data also possesses a great potential to be used for constructing, assessing and calibrating volumetric functions (Lau, et al., 2019; Sun, et al., 2016; Takoudjou et al. 2018). The general applicability of the function containing the d_6 is limited by the fact that its measurement is not a standard procedure due to its practical difficulties and has thus been excluded from, for example, current Finnish NFI.

Field measurements are given a particular role in this study, but regarding them always as the “truth” may be misleading. Instead, they have numerous potential sources of errors, and their validity should be carefully confirmed. In particular, tree height measurements contain both random as well as systematic errors (Wang, et al., 2019b) which do not necessarily derive from the measurement devices as such but from practical difficulties such as leaning trees or limited visibility to observe the treetop (Bragg, 2014; Larjavaara & Muller-Landau, 2013). Moreover, measurements also require resources allocated for the field crew, which either increase the efforts of the scanning team, or require separate trained personnel for fieldwork. Another option would be to predict tree heights by airborne laser scanning which is robust for forest conditions although uncertainties increase when measuring intermediate or suppressed trees (Wang, et al., 2019b). Diameter measurements, in turn, are sensitive to non-circularity of the stem, but also depend on the selection of the measurement height, positioning the measuring device, and reading the diameter value. These errors should not be expected to be systematic, but random deviations of several percent are likely to be

relatively common (Elzinga, et al., 2005; Päivinen, 1987). Regardless of these considerations, it is evident that field data has a high potential to rather improve than degrade the results when used to assist automatized TLS analyses.

5. Conclusions

TLS point clouds can be applied to predict stem volumes of individual trees, but the accuracy of the results mainly depends on the coverage and faultlessness of the initial point cloud data. Major factors affecting the point cloud quality are the limitations of scanner technology, scanning design and available resources; prevailing conditions such as wind; and flaws of the automatized extraction methods to detect the actual stem dimensions. Furthermore, these may lead to erroneous or biased results, particularly at higher stem densities, potentially impeding the ability to collect a representative sample over the targeted variation. A hybrid strategy, driven by the initial TLS data but assisted by additional field measurements, has, however, the potential to mitigate these errors considerably. This study indicates that even relatively simple field measurements, such as DBH and tree height, have the potential to correct large deviations in stem volume calculations at plot level, and decrease RMS errors by up to over 50%. More efforts are still required to assess the applicability and robustness of the proposed methods in different forest conditions and scan setups, as well as to gain an improved understanding on the related error sources.

CRediT authorship contribution statement

Timo P. Pitkänen: Conceptualization, Methodology, Software, Validation, Investigation, Writing - original draft, Writing - review & editing, Visualization. **Pasi Raumonen:** Methodology, Software, Writing - original draft, Writing - review & editing. **Xinlian Liang:** Methodology, Software, Validation, Investigation, Writing - review & editing. **Matti Lehtomäki:** Validation, Investigation, Writing - review & editing. **Annika Kangas:** Methodology, Writing - review & editing, Supervision.

Declaration of Competing Interest

The authors declare that they have no known competing financial interests or personal relationships that could have appeared to influence the work reported in this paper.

Acknowledgements

This work was financially supported by Finland's Ministry of Agriculture and Forestry key project "Wood on the move and new products from forests", Strategic Research Council at the Academy of Finland project "Competence-Based Growth Through Integrated Disruptive Technologies of 3D Digitalization, Robotics, Geospatial Information and Image Processing/Computing – Point Cloud Ecosystem" (project decision number 293389 / 314312), and 3DForMod project of European Union's Horizon 2020 research and innovation program ERA-NET FACCE ERA-GAS (ANR-17-EGAS-0002-01). The authors wish also to acknowledge CSC – IT Center for Science, Finland, for computational resources.

References

Abegg, M., et al., 2017. Terrestrial Laser Scanning for Forest Inventories—Tree Diameter Distribution and Scanner Location Impact on Occlusion. Forests 8, 184.
Bauwens, S., Bartholomeus, H., Calders, K., Lejeune, P., 2016. Forest Inventory with Terrestrial LiDAR: A Comparison of Static and Hand-Held Mobile Laser Scanning. Forests 7, 127.
Bazezev, M.N., Hussin, Y.A., Kloosterman, E.H., 2018. Integrating Airborne LiDAR and Terrestrial Laser Scanner forest parameters for accurate above-ground biomass/carbon estimation in Ayer Hitam tropical forest, Malaysia. Int. J. Appl. Earth Obs. Geoinf. 73, 638–652.
Béland, M., et al., 2014. On seeing the wood from the leaves and the role of voxel size in determining leaf area distribution of forests with terrestrial LiDAR. Agric. For. Meteorol. 184, 82–97.
Béland, M., et al., 2019. On promoting the use of lidar systems in forest ecosystem research. For. Ecol. Manage. 450, 117484.
Bragg, D.C., 2014. Accurately Measuring the Height of (Real) Forest Trees. J. Forest. 112, 51–54.
Bonan, G.B., 2008. Forests and Climate Change: Forcings, Feedbacks, and the Climate Benefits of Forests. Science 320, 1444–1449.
Cifuentes, R., et al., 2014. Effects of voxel size and sampling setup on the estimation of forest canopy gap fraction from terrestrial laser scanning data. Agric. For. Meteorol. 194, 230–240.
de Conto, T., Olofsson, K., Görgens, E.B., Estraviz Rodriques, L.C., Almeida, G., 2017. Performance of stem denoising and stem modelling algorithms on single tree point clouds from terrestrial laser scanning. Comput. Electron. Agric. 143, 165–176.
Côté, J.-F., Widlowski, J.-L., Fournier, R.A., Verstratete, M.M., 2009. The structural and radiative consistency of three-dimensional tree reconstructionsfrom terrestrial lidar. Remote Sens. Environ. 2009, 1067–1081.
Dassot, M., Constant, T., Fournier, M., 2011. The use of terrestrial LiDAR technology in forest science: application fields, benefits and challenges. Ann. For. Sci. 68, 959–974.
Dassot, M., Colin, A., Santenoise, P., Fournier, M., Constant, T., 2012. Terrestrial laser scanning for measuring the solid wood volume, including branches, of adult standing trees in the forest environment. Comput. Electron. Agric. 89, 86–93.
Elzinga, C., Shearer, R.C., Elzinga, G., 2005. Observer Variation in Tree Diameter Measurements. West. J. Appl. For. 20, 134–137.
Finnish Forest Research institute, 2011. State of Finland's Forests 2011 Based on the Criteria and Indicators of Sustainable Forest Management. Ministry of Agriculture and Forestry & Finnish Forest Research Institute, Helsinki.
Fischler, M.A., Bolles, R.C., 1981. Random sample consensus: A paradigm for model fitting with applications to image analysis and automated cartography. Commun. ACM 24, 381–395.
Forsman, M., et al., 2018. Bias of cylinder diameter estimation from ground-based laser scanners with different beam widths: A simulation study. ISPRS J. Photogramm. Remote Sens. 135, 84–92.
From, F., et al., 2016. Effects of simulated long-term N deposition on Picea abies and Pinus sylvestris growth in boreal forest. Can. J. For. Res. 46, 1396–1403.
Grau, E., et al., 2017. Estimation of 3D vegetation density with Terrestrial Laser Scanning data using voxels. A sensitivity analysis of influencing parameters. Remote Sens. Environ. 191, 373–388.
Griebel, A., et al., 2015. Reliability and limitations of a novel terrestrial laser scanner for daily monitoring of forest canopy dynamics. Remote Sens. Environ. 166, 205–213.
Hauglin, M., Astrup, R., Gobakken, T., Næsset, E., 2013. Estimating single-tree branch biomass of Norway spruce with terrestrial laser scanning using voxel-based and crown dimension features. Scand. J. For. Res. 28, 456–469.
Heinzel, J., Huber, M.O., 2017a. Detecting Tree Stems from Volumetric TLS Data in Forest Environments with Rich Understory. Remote Sens. 9, 9.
Heinzel, J., Huber, M.O., 2017b. Tree Stem Diameter Estimation From Volumetric TLS Image Data. Remote Sens. 9, 614.
Henttonen, H.M., Mäkinen, H., Nöjd, P., 2009. Seasonal dynamics of the radial increment of Scots pine and Norway spruce in the southern and middle boreal zones in Finland. Can. J. For. Res. 39, 606–618.
Herajärvi, H., 2001. Technical Properties of Mature Birch (Betula pendula and B. pubescens)for Saw Milling in Finland. Silva Fennica 35, 469–485.
Hosoi, F., Nakai, Y., Omasa, K., 2013. 3-D voxel-based solid modeling of a broad-leaved tree for accurate volume estimation using portable scanning lidar. ISPRS J. Photogramm. Remote Sens. 82, 41–48.
Korhonen, K.T., Maltamo, M., 1990. Männyn maanpäällisten osien kuivamassat Etelä-Suomessa. Metsäntutkimuslaituksen tiedonantoja 371. Finnish Forest Research Institute, Joensuu.
Kuronen, M., Henttonen, H.M., Myllymäki, M., 2018. Correcting for nondetection in estimating forest characteristics from single-scan terrestrial laser measurements. Can. J. For. Res. 49, 96–103.
Laasasenaho, J., 1982. Taper curve and volume functions for pine, spruce and birch. Helsinki: Finnish Forest Research Institute.
Lappi, J., 1986. Mixed linear models for analyzing and predicting stem form variation of Scots pine. Finnish Forest Research Institute, Helsinki.
Lappi, J., 2006. A multivariate, nonparametric stem-curve prediction method. Can. J. For. Res. 36, 1017–1027.
Larjavaara, M., Muller-Landau, H.C., 2013. Measuring tree height: a quantitative comparison of two common field methods in a moist tropical forest. Methods Ecol. Evol. 4, 793–801.
Lau, A., et al., 2019. Tree Biomass Equations from Terrestrial LiDAR: A Case Study in Guyana. Forests 10, 527.
Liang, X., et al., 2018. International benchmarking of terrestrial laser scanning approaches for forest inventories. ISPRS J. Photogramm. Remote Sens. 144, 137–179.
Liang, X., et al., 2016. Terrestrial laser scanning in forest inventories. ISPRS J. Photogramm. Remote Sens. 115, 63–77.
Liang, X., et al., 2014. Automated Stem Curve Measurement Using Terrestrial Laser Scanning. IEEE Trans. Geosci. Remote Sens. 52, 1739–1748.
Liu, G., et al., 2018. Estimating Individual Tree Height and Diameter at Breast Height (DBH) from Terrestrial Laser Scanning (TLS) Data at Plot Level. Forests 9, 398.
Lovell, J.L., Jupp, D.L., Newnham, G.J., Culvenor, D.S., 2011. Measuring tree stem diameters using intensity profiles from ground-based scanning lidar from a fixed viewpoint. ISPRS J. Photogramm. Remote Sens. 66, 46–55.

Luoma, V., et al., 2019. Examining Changes in Stem Taper and Volume Growth with Two-Date 3D Point Clouds. Forests 10, 382.
MATLAB, 2016. Version 9.1, (R2016b). The MathWorks Inc., Natick, Massachusetts.
McRoberts, R.E., Westfall, J.A., 2014. Effects of Uncertainty in Model Predictions of Individual Tree Volume on Large Area Volume Estimates. For. Sci. 60, 34–42.
Mengesha, T., Hawkins, M., Nieuwenhuis, M., 2015. Validation of terrestrial laser scanning data using conventional forest inventory methods. Eur. J. For. Res. 134, 211–222.
Newnham, G.J., et al., 2015. Terrestrial Laser Scanning for Plot-Scale Forest Measurement. Curr. Forestry Reports 1, 239–251.
Nölke, N., et al., 2015. On the geometry and allometry of big-buttressed trees - a challenge for forest monitoring: new insights from 3D-modeling with terrestrial laser scanning. *iForest* – Biogeosci. Forestry 8, 574–581.
Ojoatre, S., et al., 2019. Assessing the uncertainty of tree height and Aboveground Biomass from Terrestrial Laser Scanner and Hypsometer using Airborne LiDAR data in Tropical rainforests. IEEE J. Sel. Top. Appl. Earth Obs. Remote Sens. 12, 4149–4159.
Olschofsky, K., Mues, V., Köhl, M., 2016. Operational assessment of aboveground tree volume and biomass by terrestrial laser scanning. Comput. Electron. Agric. 127, 699–707.
Paláncz, B., et al., 2016. A robust cylindrical fitting to point cloud data. Aust. J. Earth Sci. 63, 665–673.
Patenaude, G., Milne, R., Dawson, T.P., 2005. Synthesis of remote sensing approaches for forest carbon estimation: reporting to the Kyoto Protocol. Environ. Sci. Policy 8, 161–178.
Pitkänen, T.P., Raumonen, P., Kangas, A., 2019. Measuring stem diameters with TLS in boreal forests by complementary fitting procedure. ISPRS J. Photogramm. Remote Sens. 147, 294–306.
Pueschel, P., et al., 2013. The influence of scan mode and circle fitting on tree stem detection, stem diameter and volume extraction from terrestrial laser scans. ISPRS J. Photogramm. Remote Sens. 77, 44–56.
Pyörälä, J., et al., 2018. Quantitative Assessment of Scots Pine (Pinus Sylvestris L.) Whorl Structure in a Forest Environment Using Terrestrial Laser Scanning. IEEE J. Sel. Top. Appl. Earth Obs. Remote Sens. 11, 3598–3607.
Päivinen, R., 1987. A planning model for forest inventory (English Summary). University of Joensuu, Joensuu.
R Core Team, 2016. R: A language and environment for statistical computing. R Foundation for Statistical Computing, Vienna, Austria https://www.r-project.org/ (accessed 24 February 2020).
Raumonen, P., et al., 2015. Massive-scale Tree Modelling from TLS Data. ISPRS Ann. Photogram., Remote Sens. Spat. Inf. Sci. II-3/W4, 189–196.
Reddy, R.S., Jha, C.S., Rajan, K.S., 2018. Automatic Tree Identification and Diameter Estimation Using Single Scan Terrestrial Laser Scanner Data in Central Indian Forests. J. Indian Soc. Remote Sens. 46, 937–943.
Saarinen, N. et al., 2019a. Assessing the effects of thinning on stem growth allocation of individual Scots pine trees. Forest Ecology and Management, 474, p. 118344.
Saarinen, N. et al., 2019b. Assessing the Effects of Sample Size on Parametrizing a Taper Curve Equation and the Resultant Stem-Volume Estimates. Forests, 10, p. 848.
Saarinen, N., et al., 2017. Feasibility of Terrestrial laser scanning for collecting stem volume information from single trees. ISPRS J. Photogramm. Remote Sens. 123, 140–158.
Schmitz, A., et al., 2018. Responses of forest ecosystems in Europe to decreasing nitrogen deposition. Environ. Pollut. 244, 980–994.
Schneider, R., et al., 2018. Climate-induced changes in the stem form of 5 North American tree species. For. Ecol. Manage. 427, 446–455.
Seidel, D., et al., 2013. Using terrestrial laser scanning to support biomass estimation in densely stocked young tree plantations. Int. J. Remote Sens. 34, 8699–8709.
Seidel, D., Ehbrecht, M., Puettman, K., 2016. Assessing different components of three-dimensional forest structure with single-scan terrestrial laser scanning: A case study. For. Ecol. Manage. 381, 196–208.
Srinivasan, S., et al., 2015. Terrestrial Laser Scanning as an Effective Tool to Retrieve Tree Level Height, Crown Width, and Stem Diameter. Remote Sens. 7, 1877–1896.
Sun, Y., et al., 2016. Deriving Merchantable Volume in Poplar through a Localized Tapering Function from Non-Destructive Terrestrial Laser Scanning. Forests 7, 87.
Takoudjou, S.M., et al., 2018. Using terrestrial laser scanning data to estimate large tropical trees biomass and calibrate allometric models: A comparison with traditional destructive approach. Methods Ecol. Evol. 9, 905–916.
Tomppo, E., et al., 2011. Designing and Conducting a Forest Inventory - case: 9th National Forest Inventory of Finland. Springer, Dordrecth.
Vaaja, M., et al., 2016. The Effect of Wind on Tree Stem Parameter Estimation Using Terrestial Laser Scanning. ISPRS Annals of the Photogrammetry, Remote Sensing and Spatial Information Sciences, III-8, pp. 117–122.
Wang, D., et al., 2017. Reconstructing Stem Cross Section Shapes From Terrestrial Laser Scanning. IEEE Geosci. Remote Sens. Lett. 14, 272–276.
Wang, Y., et al., 2019a. Is field-measured tree height as reliable as believed – A comparison study of tree height estimates from field measurement, airborne laser scanning and terrestrial laser scanning in a boreal forest. ISPRS J. Photogramm. Remote Sens. 147, 132–145.
Wang, Y., et al., 2019b. In situ biomass estimation at tree and plot levels: What did data record and what did algorithms derive from terrestrial and aerial point clouds in boreal forest. Remote Sens. Environ. 232, 111309.
Varjo, J., et al., 2006. Digital horizontal tree measurements forforest inventory. Finnish Forest Research Institute, Helsinki.
Vaunkonen, J., Packalen, T., 2018. Uncertainties related to climate change and forest management with implications on climate regulation in Finland. Ecosyst. Serv. 33, 213–224.
Verkasalo, E., 1997. Hieskoivun laatu vaneripuuna (in Finnish). Metsäntutkimuslaitoksen tiedonantoja 632. Metla, Joensuu.
West, P.W., 2015. Stem Volume and Taper Functions. In: Tree and Forest Measurement. Springer, Cham, pp. 37–51.
White, J.C., et al., 2016. Remote Sensing Technologies for Enhancing Forest Inventories: A Review. Can. J. Remote Sens. 42, 619–641.
Wilkes, P., et al., 2017. Data acquisition considerations for Terrestrial Laser Scanning of forest plots. Remote Sens. Environ. 196, 140–153.
Yrttimaa, T., et al., 2020. Multisensorial Close-Range Sensing Generates Benefits for Characterization of Managed Scots Pine (Pinus sylvestris L.) Stands. ISPRS J. Geo-Inform. 9, 309.
Zianis, D., Muukkonen, P., Mäkipää, R. & Mencuccini, M., 2005. Biomass and Stem Volume Equations for Tree Species in Europe. Silva Fennica Monographs 4. Helsinki: The Finnish Society of Forest Science and The Finnish Forest Research Institute.
Åkerblom, M., Raumonen, P., Kaasalainen, M., Casella, E., 2015. Analysis of Geometric Primitives in Quantitative Structure Models of Tree Stems. Remote Sens. 7, 4581–4603.